International Journal of Heat and Mass Transfer 52 (2009) 2925–2931

Contents lists available at ScienceDirect

International Journal of Heat and Mass Transfer

journal homepage: www.elsevier.com/locate/ijhmt

Enhanced flow boiling heat transfer of FC-72 on micro-pin-finned surfaces

Aixiang Ma, Jinjia Wei *, Minzhe Yuan, Jiabin Fang

State Key Laboratory of Multiphase Flow in Power Engineering, Xi'an Jiaotong University, Xi'an 710049, China

ARTICLE INFO

Article history:
Received 1 August 2008
Received in revised form 16 February 2009
Accepted 17 February 2009
Available online 1 April 2009

Keywords:
Flow boiling heat transfer
Electronic cooling
High heat flux
Micro-pin-fin
FC-72

ABSTRACT

For the purpose of cooling electronic components with high heat flux efficiently, some experiments were conducted to study the flow boiling heat transfer performance of FC-72 on silicon chips. Micro-pin-fins were fabricated on the chip surface using a dry etching technique to enhance boiling heat transfer. Three different fluid velocities (0.5, 1 and 2 m/s) and three different liquid subcoolings (15, 25 and 35 K) were performed, respectively. A smooth chip (chip S) and four micro-pin-finned chips with the same fin thickness of 30 μm and different fin heights of 60 μm (chip PF30–60) and 120 μm (chip PF30–120), respectively, were tested. All the micro-pin-finned surfaces show a considerable heat transfer enhancement compared to the smooth one, and the critical heat flux increases in the order of chip S, PF30–60 and PF30–120. For a lower ratio of fin height to fin pitch and/or higher fluid velocity, the fluid velocity has a positive effect on the nucleate boiling curves for the micro-pin-finned surfaces. At the velocities lower than 1 m/s, the micro-pin-finned surfaces show a sharp increase in heat flux with increasing wall superheat, and the wall temperature at the critical heat flux (CHF) is less than the upper limit, 85 °C, for the reliable operation of LSI chips. The CHF values for all surfaces increase with fluid velocity and subcooling. The maximum CHF can reach nearly 150 W/cm^2 for chip PF30–120 at the fluid velocity of 2 m/s and the liquid subcooling of 35 K.

© 2009 Elsevier Ltd. All rights reserved.

1. Introduction

With increasing development of the IC (integrated circuits) technology, the size of electronic circuit is being significantly reduced, and the integrated circuit densities in chips are substantially increasing, resulting in a rapid increasing of power dissipation rate at the chip, module and system levels. Sophisticated electronic cooling technology is needed to maintain a relatively constant component temperature below the junction temperature, approximately 85 °C for most mainframe memory and logic chips.

Direct liquid cooling with phase change using dielectric fluids such as FC-72 is a prospective scheme for high-powered electronic devices. But the drawbacks of dielectric fluids are the high wetting behavior and the poor thermal transfer properties compared to the common fluids such as water, which causes unusually high incipient boiling superheat and relatively small value of the critical heat flux (CHF). Fabrication of microstructures on the chip surfaces can effectively enhance boiling heat transfer. Since 1970s, a number of studies have dealt with the enhancement of boiling heat transfer from electronic components by use of treated surfaces. These include a sand-blasted and KOH-treated surface [1], a dendritic heat sink (a brush-like structure) [1,2], laser-drilled holes (3–15 μm in mouth diameter) [3], re-entrant cavities (0.23–0.5 μm in mouth diameter) [4], spraying and painting of alumina particle (0.3–5 μm in diameter) or diamond particle (1–12 μm in diameter) [5], heat sink studs with drilled holes, micro-fins with and without microporous coating, micro-channels and pores, etc. (0.2–12 mm in feature size) [6], micro-re-entrant cavities (1–3 μm in mouth diameter) [7]. All the above treated surfaces show the drawback of severe deterioration in boiling heat transfer in the high heat flux region, and the wall temperature at CHF is higher than the upper limit, 85 °C, for the reliable operation of LSI chips. Mudawar's group [8] studied the nucleate pool boiling enhancement by using carbon nanotube (CNT) arrays and found CNTs were quite effective in reducing incipient superheat and enhancing the boiling heat transfer coefficient. However, it is still a challenge to increase CHF by a large margin concerning this treated surface for the application of cooling on the high-heat-flux chip.

Honda and Wei [9–12] made noticeable progress in nucleate boiling enhancement by using micro-pin-fins (10–50 μm in thickness and 60–200 μm in height) fabricated by dry etching. From the boiling incipience to the critical heat flux, the temperature of the micro-pin-finned surfaces almost did not increase with the heat flux. The increase of CHF could reach more than twice that of a smooth chip, and the wall temperature at the CHF point was lower than 85 °C. The micro-pin-finned surface appeared to be one promising enhanced surface for cooling schemes of electronic components. However, the micro-pin-finned surface was only tested in a pool of FC-72, and its enhancement ability under flow boiling

* Corresponding author. Tel.: +86 29 82664462.
E-mail address: jjwei@mail.xjtu.edu.cn (J. Wei).

0017-9310/$ - see front matter © 2009 Elsevier Ltd. All rights reserved.
doi:10.1016/j.ijheatmasstransfer.2009.02.031

Nomenclature

A	projected surface area of chip (cm^2)	T_b	temperature of bulk liquid (°C)
A_t	total surface area of micro-pin-finned chip (cm^2)	T_{sat}	saturation temperature (°C)
h	fin height (μm)	T_w	wall temperature (°C)
p	fin pitch (μm)	t	fin thickness (μm)
q	heat flux based on projected surface area (W/cm^2)	V	fluid velocity (m/s)
q_c	single-phase, forced convection heat flux (W/cm^2)	ΔT_b	wall superheat = $T_w - T_b$ (K)
q_{CHF}	critical heat flux (W/cm^2)	ΔT_{sat}	wall superheat = $T_w - T_{sat}$ (K)
q_{cS}	single-phase, forced convection heat flux of smooth surface (W/cm^2)	ΔT_{sub}	liquid subcooling = $T_{sat} - T_b$ (K)

was not yet revealed. Some researchers, such as Mudawar and Maddox [13], Kutateladze and Burakov [14], Samant and Simon [15] and Rainey and You [16], have found that both fluid velocity and subcooling had significant positive effects on the nucleate boiling curve and the critical heat flux of their thin film heater. Therefore, the objective of this paper is to study the combined effects of fluid velocity and subcooling on the flow boiling heat transfer of FC-72 over micro-pin-finned surfaces for further enhancement of boiling heat transfer to cool high-heat-flux devices. Two micro-pin-finned chips with the same fin thickness of 30 μm and different fin heights of 60 μm (chip PF30–60) and 120 μm (chip PF30–120), respectively, were tested. A smooth one was also tested for comparison.

2. Experimental apparatus and procedures

The flow boiling test facility used for the present study is shown schematically in Fig. 1. It is a closed-loop circuit consisting of a tank, a scroll pump, a test section, two heat exchangers and a turbine flowmeter. The tank serves as a fluid reservoir and pressure regulator during testing. The condenser before the pump is used to cool the fluid and prevent cavitation in the pump. The pre-heater before the test section is used to control the inlet temperature of test section. The pump is combined with a converter to control the mass flow rate. To ensure proper inlet pressure control, a pressure transducer is installed at the inlet of the test section. The pressure drop across the test section is also measured by a pressure-difference transducer. The flowmeter and the sensors for pressure and pressure difference have the function of outputting 4–20 mA current signals and are measured directly by a data acquisition system.

The test chip is a P-doped N-type square silicon chip with the side length of 10 mm and the thickness of 0.5 mm. The chip is bonded to a substrate made of polycarbonate using epoxy adhesive and fixed in the horizontal, upward facing orientation on the bottom surface of a 5 mm high and 30 mm wide horizontal channel as shown in Fig. 2(a). The chip is located 300 mm (60 hydraulic diameter) from the inlet of the test section so that the fluid flow on it is estimated to be fully developed turbulent flow within the range of present fluid velocity. The side surfaces of the chip are covered with adhesive to minimize heat loss. Therefore, only the upper surface of the chip is effective for heat transfer. The chip is Joule heated by using a DC power supply. The details of the heater assembly are shown in Fig. 2(b). Two 0.25 mm diameter copper wires for the power supply and voltage drop measurement are soldered by a low temperature solder (the melting point of 180 °C) to the side surfaces at the opposite end. In order to secure the Ohmic contact between the test chip and the copper wires, a special solder

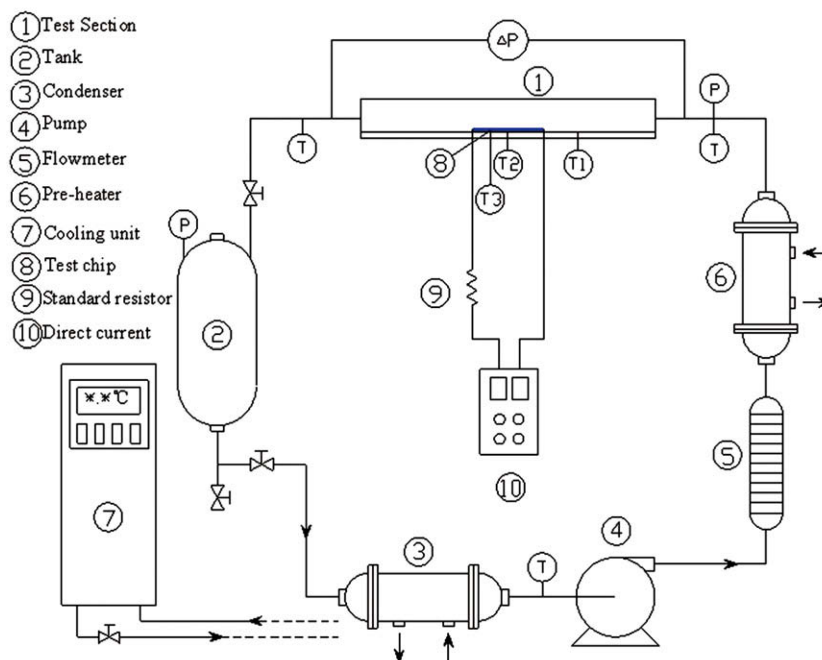

Fig. 1. Flow boiling test loop.

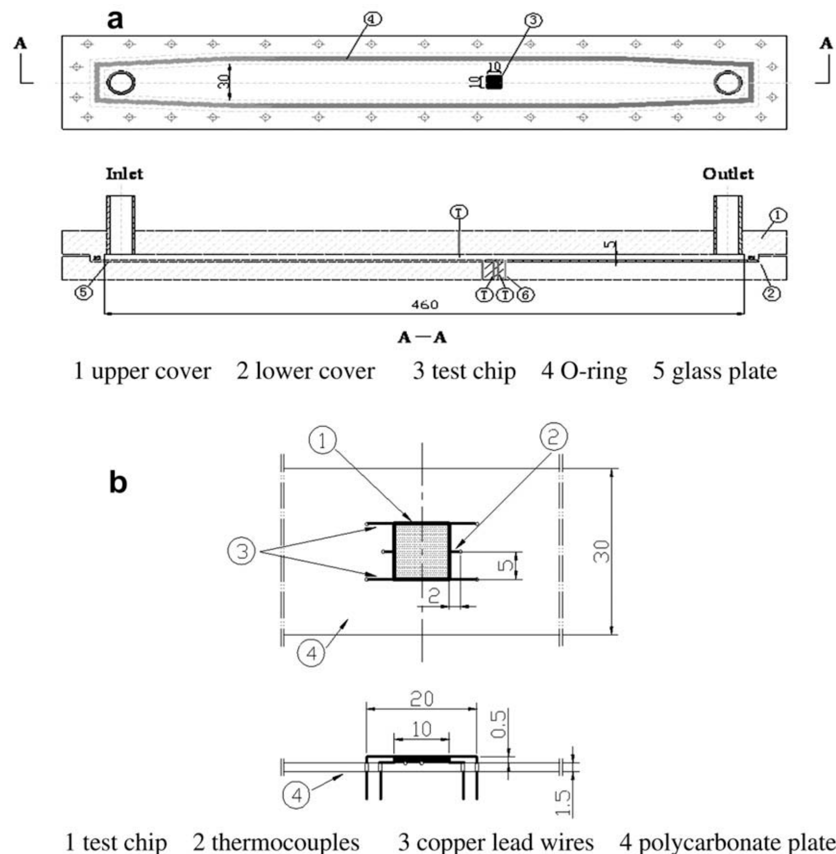

Fig. 2. Schematic diagram of test section and heater assembly. (a) Test section. (b) Details of heater assembly.

with the melting point of 300 °C is applied to the chip with ultrasonic bonding method before soldering the copper wires. The power supply is connected to a standard resistor (1 Ω) and the test chip. The standard resistor is used to measure the current in the circuit. To measure chip temperature, two 0.12 mm diameter T-type thermocouples for measuring the local wall temperature are adhered under the test chip at the center and at about 1.5 mm from the downstream end. A data acquisition unit is connected to a personal computer that automatically converts the output voltages of thermocouples into temperatures. Then the voltage drops of the test chip and the standard resistor are read and recorded for eight times, and average values of these measurements are adopted as experimental data.

The test channel, where the test chip is fixed at the bottom, is made of Pyrex glass for visualizing flow boiling phenomena using a high speed video. To prevent the liquid from leaking out, the upper and nether covers are fastened by bolts and sealed with an O-ring. The local temperature of test liquid at the chip level is measured by a T-type thermocouple, whose hot junction is located in a vertical line 25 mm away from the edge of test chip. The measured temperature is used as the bulk temperature of test fluid, T_b.

FC-72 is used as the working fluid. A pressurized air is bubbled into the test liquid for about 12 h, and then the test liquid is exposed to ambient air for 12 h. The mole fraction of dissolved air is measured by a gas chromatograph, and the measured value is about 3×10^{-3}, which is almost unchanged before and after a series of experiments. The experiments are performed at three fluid velocities (0.5, 1 and 2 m/s) and for three liquid subcoolings (15, 25 and 35 K). The fluid in the test channel is kept at one atmospheric pressure. For the enhancement of boiling heat transfer, micro-pin-fins with square cross-sections are fabricated on the surface of silicon chip using the dry etching technique. To study the effects of the height of micro-pin-fin, tests are carried out on the micro-pin-finned chips with the same fin thickness of t = 30 μm and different fin heights of h = 60, 120 μm, respectively. The fin pitch p is twice the fin thickness. The scanning-electron-microscope (SEM) images of chips PF30–60 and PF30–120 are shown in Fig. 3(a) and (b), respectively. A smooth chip is also tested for comparison.

After FC-72 is infused, a frequency converter is adjusted to make the pump work at a required fixed mass flow rate. Then a cooling unit is run to control the liquid temperature in the channels. When the loop reaches steady state, the power supply is initiated to heat the test chip. A short delay is imposed before initiation of data acquisition to make sure that the steady-state condition is attained. Power input to the test chip is increased in small steps up to the high heat flux region of nucleate boiling. The heat flux q is obtained from the voltage drop of the test chip and the current. An overheating protection system is incorporated in the power circuit. If the wall temperature sharply increases by more than 20 K in a short time, the data acquisition algorithm will assume the occurrence of CHF condition, and the power supply will be immediately shut down. The CHF value is computed as the steady-state heat flux value just prior to the shutdown of power supply.

Experimental uncertainties are estimated using the method of Kline and McClintock [17]. The uncertainties in the chip and bulk liquid temperature measurements by the thermocouples are estimated to be less than 0.3 K. Wall temperature uncertainty can be attributed to the errors caused by thermocouple calibration by a platinum resistance thermometer (0.03 K), temperature correction for obtaining surface temperature from the measured value at the bottom of the chip (0.2 K), the temperature unsteadiness (0.1 K) and the thermocouple resolution (less than 0.1 K). The uncertainty

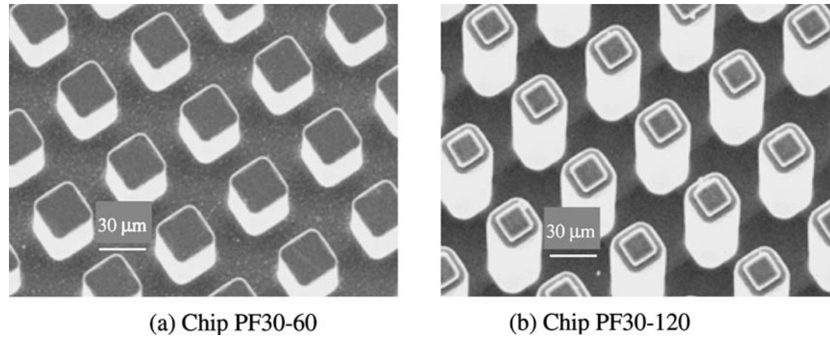

Fig. 3. SEM images of micro-pin-fins.

of the bulk temperature is due to errors caused by thermocouple calibration by a platinum resistance thermometer (0.03 K), the temperature unsteadiness (0.2 K) and the thermocouple resolution (less than 0.1 K). Heat flux uncertainty includes the error of electric power supplied to the chip (0.11%), which is calculated from the errors of the current (0.014%) and voltage (0.1%) across the chip and heat loss by substrate heat conduction. The heat loss is estimated by solving three-dimensional conduction problems through substrate using a commercial software FLUENT with the measured wall temperature as a given condition, which is less than 16% and 6% for the forced convection and the nucleate boiling regions, respectively. It should be mentioned that q includes the heat transferred to the bulk liquid by conduction through the polycarbonate substrate.

3. Results and discussion

Fig. 4 shows the flow boiling curves of the smooth surface chip S. The locations of the onset of nucleate boiling (ONB) and the CHF are indicated by arrows in the figure. The single-phase, forced convection data clearly shows the effects of fluid velocity. For comparison, the correlation of single-phase forced convection heat transfer proposed by Gersey and Mudawar [18] at $V = 0.5$ m/s is also shown in Fig. 4. The measured heat flux in the non-boiling region is about 20% higher than the correlation mainly due to the heat loss caused by conduction through the copper lead wires and the glass substrate and some uncertainties of the correlation itself. For a given fluid subcooling, the nucleate boiling curves almost collapse to one line, indicating that the heat transfer performance is dominated by the nucleate boiling heat transfer, and the critical heat flux increase as the fluid velocity is increased. By plotting the boiling curves with ΔT_b, the effect of fluid subcooling on the nucleate boiling heat transfer appears to be directly related to subcooling level. The critical heat flux also increases with increasing fluid subcooling at a given fluid velocity. The pool boiling curve for chip S at $\Delta T_{\mathrm{sub}} = 25$ K is also shown in Fig. 4 for comparison. It can be seen that the boiling curve of smooth surface is significantly shifted to the right compared to the flow boiling curve at $\Delta T_{\mathrm{sub}} = 25$ K. This suggests that the fluid velocity has a significant effect on the boiling heat transfer performance in the low velocity range of 0–0.5 m/s. This phenomenon was also observed by Rainey et al. [16]. Using a highly polished thin gold film heater in R-113, Kirk et al. [19] found that increasing fluid velocity from 0.041 to 0.325 m/s significantly shifted the entire nucleate boiling curve to the left by about 5 K.

The flow boiling curves of chip PF30–60 are shown in Fig. 5. The single-phase, forced convection curves of the micro-pin-finned surface show much higher heat flux than those of the smooth surface as shown in Fig. 4, indicating that the side walls of micro-pin-fins are exposed to the fluid flow and are active for the forced convection heat transfer. This is different from the natural convection heat transfer in the pool boiling data of Wei and Honda [10], where the natural convection curves are not impacted by the micro-pin-fins since they are completely submerged in the thermal boundary layer of superheated liquid. In the nucleate boiling region, we can see that the boiling curves are greatly affected by fluid velocity, and the wall superheat decreases with increasing fluid velocity at the same heat flux. This indicates that the forced convection also play a very important role in the total heat transfer not only the nucleate boiling heat transfer. The slope of the boiling curve decreases with increasing fluid velocity, indicating that the proportion of forced convection increases with fluid velocity. Especially at the fluid velocity of 2 m/s, the slope of the nucleate boiling curves is only slightly larger than that of the forced convection heat

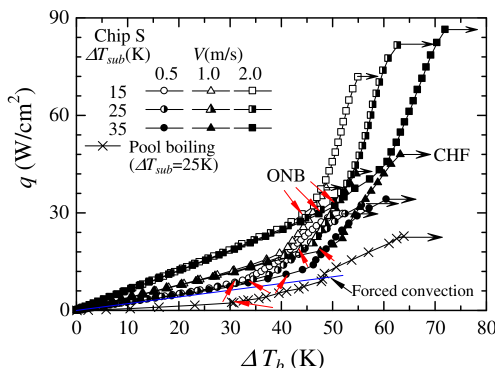

Fig. 4. Flow boiling curves of chip S.

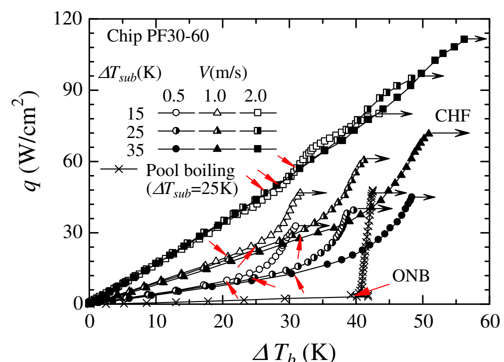

Fig. 5. Flow boiling curves of chip PF30–60.

transfer ones, showing that the forced convection dominates the heat transfer performance. The nucleate boiling curves for the fluid velocities of 0.5 and 1 m/s can be correlated with the following equation:

$$q = a\Delta T_b^n \quad (1)$$

The values of coefficient a and exponent n are shown in Table 1.

For the micro-pin-finned surface, the ratio of fin height to fin pitch, h/p, and the fluid velocity are key parameters for determining the boiling heat transfer. When h/p is very small and/or the fluid velocity is very large, the bubble nucleation on the bottom and side wall surfaces of the micro-pin-fin is easily impacted by the forced flow over the chip surface, which prevents the burst of nucleate bubbles and thus reduces the proportion of nucleate boiling heat transfer. Fig. 6 shows flow boiling phenomena of chip PF30–60 at $q = 38$ W/cm^2 and $V = 1$ m/s. We can clearly see that the bubbles are not occupied fully on the chip surface, and the proportion of bubble area decreases with increasing fluid subcooling. This shows that there exists a certain proportion of heat transfer area for single-phase, forced convection heat transfer, and thus the boiling heat transfer is greatly affected by fluid velocity. In pool boiling, we also find that for the lowest $h/p = 0.6$ ($t = 50$ μm, $h = 60$ μm), the bubble nucleation is affected by the local fluid flow and heat transfer on the chip surface, and the slope of the boiling curve in the fully developed nucleate boiling region is smaller than those of the other micro-pin-finned chips [10]. The pool boiling curve of chip PF30–60 at $\Delta T_{sub} = 25$ K is also shown in Fig. 5 for comparison. The large effect of fluid velocity leads to a large deviation of the pool boiling curve from the flow boiling curves at $\Delta T_{sub} = 25$ K. Different from the smooth surface as shown in Fig. 4, the slope of the pool boiling curve for chip PF30–60 is much larger than that of the flow boiling curve. As explained by Wei et al. [12], the micro-convection and the thin liquid layer evaporation due to the bubbles generated in the gap between micro-pin-fins are the reason for the significant enhancement of pool boiling heat transfer. For the micro-pin-finned surface with a lower h/p, the bubble nucleation is largely affected by the fluid flow, reducing the boiling heat transfer enhancement. It can be seen in Fig. 5 that the CHF at 0.5 m/s and 25 K of the flow boiling is even lower than that of the pool boiling.

Fig. 7 shows the flow boiling curves of the micro-pin-finned surface with a larger fin height of 120 μm, chip PF30–120. The single-phase convective heat transfer is better than that of chip PF30–60 due to the larger heat transfer surface area. The value of h/p is 2 and 1 for chips PF30–120 and PF30–60, respectively. Therefore, the effect of fluid velocity on boiling curves of chip PF30–120 is smaller than that on chip PF30–60. We can see that at the fluid velocity less than 2 m/s, the nucleate boiling curves almost follow one line for a given liquid subcooling, showing a certain insensitivity of the nucleate boiling heat transfer to fluid velocity. The lines indicated in Fig. 7 for representing the nucleate boiling curves approximately can be expressed as:

$$q = k\Delta T_b + c \quad (2)$$

The slope k has the same value of 13.5 for the three liquid subcoolings, and the value of the intercept c is −341.0, −431.0 and −551.0 for the liquid subcoolings of 15, 25 and 35 K, respectively.

It is supposed that in case of lower fluid velocity and larger h/p, the bubble nucleation is not affected by the fluid flow on the chip surface remarkably, and hence the nucleate boiling dominates the whole heat transfer performance. At the larger fluid velocity of 2 m/s, the fluid flow and heat transfer shows great effects on bubble nucleation on the bottom and side wall surfaces, suppressing the bubble generation, reducing the stay time of bubbles and blowing them away immediately to the downstream edge after their emission, thus creating a domination of forced convection heat transfer. We can see that the slope of boiling curve is almost the same as that of the forced convection curve, showing that the forced convection heat transfer takes a very large proportion. Observation on the boiling phenomena of chips PF30–60 and PF30–120 at 2 m/s shows that the entire heated surface is not fully covered with bubbles. The bubbles from the upstream part of the heated surface are washed away by fluid flow and then combine with those from the downstream part of the heated surface to form secondary bubbles. Therefore, a large percent of bubbles assemble in the downstream part of the surface. This flow boiling phenome-

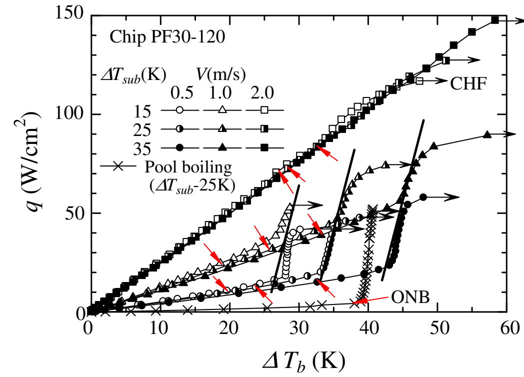

Fig. 7. Flow boiling curves of chip PF30–120.

Table 1
The values of a and n in Eq. (1) for chip PF30–60.

	$\Delta T_{sub} = 15$ K		$\Delta T_{sub} = 25$ K		$\Delta T_{sub} = 35$ K	
	a	n	a	n	a	n
$V = 0.5$ m/s	1.18×10^{-6}	5.00	5.56×10^{-7}	4.92	2.14×10^{-7}	4.93
$V = 1.0$ m/s	5.99×10^{-4}	3.26	2.55×10^{-4}	3.33	1.56×10^{-4}	3.32

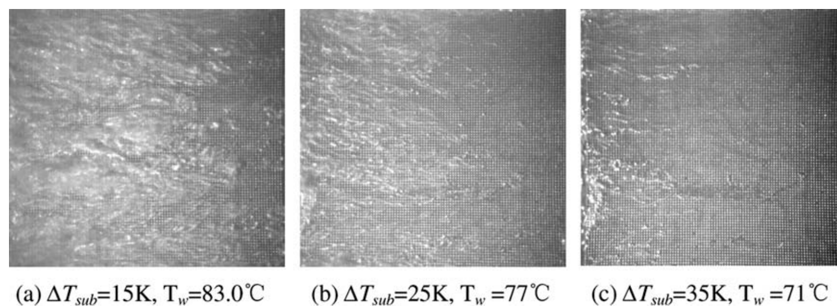

Fig. 6. Flow boiling phenomena on chip PF30–60 for different fluid subcoolings with $V = 1$ m/s, $q = 38$ W/cm^2.

non indicates that the effect of single-phase convective heat transfer still exists, and here the deterioration of heat transfer is due to local dryout of the downstream part of the test surface. The pool boiling curve of chip PF30–120 at ΔT_{sub} = 25 K is also shown in Fig. 7 for comparison. The large deviation of the pool boiling curve from the flow boiling curves at ΔT_{sub} = 25 K suggests the fluid velocity has an obvious effect in the range of 0–0.5 m/s. Different from chip PF30–60 as shown in Fig. 5, the slope of the flow boiling curve is only a little smaller than that of the pool boiling curve, showing a small fluid velocity effect on chip PF30–120 compared to chip PF30–60.

To investigate the effectiveness of micro-pin-fin on the forced convection heat transfer, the dimensionless quantity, $(q_c/q_{cS})/(A_t/A)$, in the single-phase, forced convection region for chips PF30–60 and PF30–120 is plotted as a function of V in Fig. 8. The value of $(q_c/q_{cS})/(A_t/A)$ is obtained at the same ΔT_b of 10 K. If all parts of the micro-pin-finned surface are equally effective for the convective heat transfer, the value of $(q_c/q_{cS})/(A_t/A)$ should be equal to unity irrespective of V. It can be clearly seen that $(q_c/q_{cS})/(A_t/A)$ increases with increasing fluid velocity and is higher for chip PF30–60 with smaller h/p of 1. This agrees with the aforementioned explanation that when h/p is very small and/or the fluid velocity is very large, the heat transfer of the micro-pin-fin is easily affected by the forced flow on the chip surface.

Fig. 9 shows the comparison between the boiling curves for all surfaces at ΔT_{sub} = 25 K. It can be seen that the slopes of boiling curves and the critical heat fluxes increase in the order of chip S, PF30–60 and PF30–120 at the same velocity, showing that all the micro-pin-finned surfaces have considerable heat transfer enhancement compared to a smooth one. The enhancement of heat transfer is considered as surface area increase of the micro-pin-finned chip over a smooth surface, and the surface area of micro-pin-finned chip is further enhanced by changing the height of micro-pin-fins. The growth and movement of the bubbles in the confined gaps between fins can bring about micro-convection and form thin liquid layer for evaporation, which makes the profile of fins become effective heat transfer area, creating heat transfer enhancement. Observation on boiling phenomena on the micro-pin-finned chip reveals that this surface can create more active nucleation sites and make the bubbles rest on the surface for a longer time to evaporate, thus increasing the heat transfer performance. The wall superheats decrease in the order of chip S, PF30–60 and PF30–120, and the wall temperature at the CHF point is less than the upper limit, 85 °C, for the reliable operation of LSI chips, showing that the heat transfer can be further enhanced by increasing fin height again. For comparison, Rainey et al.'s boiling curve with the liquid subcooling of 20 K for the smooth surface at 0.5 m/s and the microporous surface at 2 m/s [16] are also shown in Fig. 9. The boiling curve of the smooth surface of Rainey et al. agrees well with the present data except for a lower CHF value due to the lower liquid subcooling. The single-phase, forced convection curve of the microporous surface is worse than that of the smooth surface, chip S, at the same velocity of 2 m/s, mainly due to the lower effective thermal conductivity of the microporous coating layer as explained by Rainey et al. [16]. Although with an earlier boiling incipience, the microporous surface shows a larger wall superheat than the micro-pin-finned surfaces in the nucleate boiling region, and the heat flux at 85 °C is less than half the CHF of chip PF30–120. Comparison of the boiling curves with those of Rainey et al. [16] also shows that there is no obvious overshoot at boiling incipience. The reason is that we used gas dissolved FC-72 while Rainey et al. [16] used degassed FC-72. Our previous experiments showed that gas contents only affect the boiling curves near the boiling incipience, and the overshoot decreased or diminished for gas dissolved case [9–12].

From Figs. 5, 7 and 9, we can see that the CHF increases with both fluid velocity and subcooling. To reveal this relationship, we plot the CHF versus fluid velocity for chip S, PF30–60 and PF30–120 with fluid subcooling as a parameter in Fig. 10. The fluid velocity has a great effect on CHF. For the low fluid subcooling of 15 K and the velocity larger than 1 m/s, the rate of CHF enhancement is increased remarkably, which was also supported by many researchers such as Mudawar and Maddox [13], Rainey et al. [16], etc., who had noted that the transition from low to high velocities was characterized by an increase in the rate of CHF enhancement with velocity. However, for the large liquid subcoolings of 25

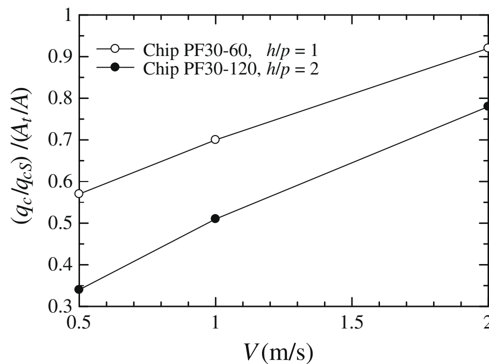

Fig. 8. Variation of $(q_c/q_{cS})/(A_t/A)$ with V.

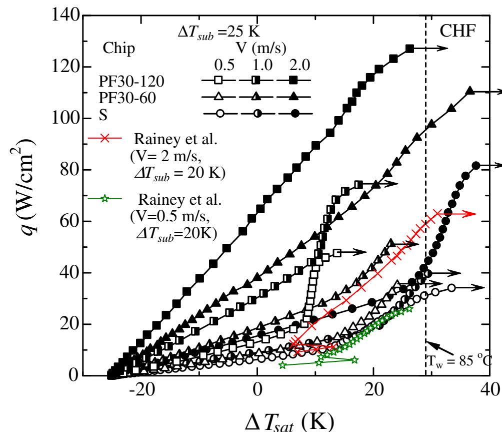

Fig. 9. Comparison of boiling curves for all chips at ΔT_{sub} = 25 K.

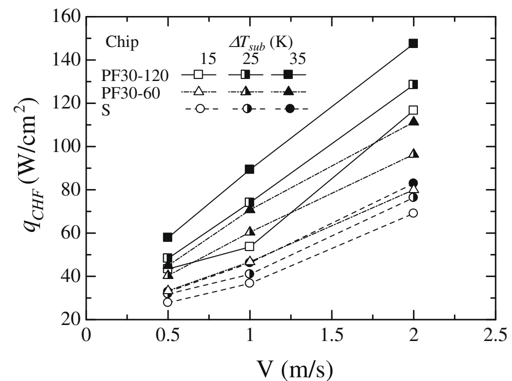

Fig. 10. Effect of fluid velocities and subcoolings on CHF.

and 35 K, there is no such obvious transition. For a low fluid subcooling, as explained by Mudawar and Maddox [13], the low velocity CHF is caused by dryout of the liquid sublayer beneath a large continuous vapor blanket near to the downstream edge of the heater; however, in the high velocity CHF regime, the thin vapor layer covering the surface is broken into continuous vapor blankets much smaller than the heater surface, decreasing the resistance of fluid flow to rewet the liquid sublayer and thus providing an additional enhancement to CHF and subsequent increase in slope. For a large fluid subcooling, the bubble size becomes small, and the heater surface is not fully occupied with the vapor layer within the range of fluid velocity in this study. Therefore, there is no obvious slope change as seen in Fig. 10. Moreover, from the slopes of boiling curves, we can see that the effect of the fluid velocity on micro-pin-finned surfaces is more noticeably compared to a smooth one, and the enhancement of CHF sharply increases with fluid velocity. For chip PF30–120, the CHF reaches nearly 150 W/cm^2 at 2 m/s and 35 K.

4. Conclusions

The flow boiling heat transfer performance of FC-72 on simulated silicon chips with micro-pin-finned surface was studied by investigating the effects of fluid velocity, subcooling and fin height. A smooth surface was also tested for comparison. The main conclusions can be summarized as follows:

(1) All micro-pin-finned surfaces have considerable heat transfer enhancement compared to a smooth one, and the slopes of boiling curves and the critical heat fluxes increase in the order of chip S, PF30–60 and PF30–120 for the same fluid velocity and subcooling, indicating that the heat transfer can be further enhanced by increasing fin height.

(2) The CHF values for all surfaces increase with fluid velocity and subcooling, and the effect of fluid velocity is more notable, especially for the fluid velocity larger than 1 m/s. The CHF of the micro-pin-finned surfaces is more sensitive to the fluid velocity and liquid subcooling than that of the smooth chip, and the maximum CHF can reach nearly 150 W/cm^2 for chip PF30–120 at the fluid velocity of 2 m/s and the liquid subcooling of 35 K. The wall temperature for the micro-pin-finned surfaces is lower than the upper temperature limit, 85 °C, for the normal operation of LSI chip.

(3) For a lower ratio of fin height to fin pitch and/or higher fluid velocity, the forced flow and heat transfer on the chip have a great effect on the bubble nucleation, and the entire micro-pin-finned surface is not completely covered with bubbles, creating a dominant convective heat transfer effect in the nucleate boiling region.

Acknowledgements

This work is supported by the key project of State Education Ministry of China (No. 106142) and the program for new century excellent talents in university (NCET-07-0680). The project is also sponsored by the National Fundamental Research Program of China (No. 2006CB601203).

References

[1] S. Oktay, Departure from natural convection (DNC) in low-temperature boiling heat transfer encounted in cooling micro-electronic LSI devices, in: Proceeding of 7th International Heat Transfer Conference, Munich, vol. 4, 1982, pp. 113–118.
[2] S. Oktay, A. Schmekenbecher, Method for Forming Heat Sinks on Semiconductor Device Chips, U.S. Patent No. 3706127, 1972.
[3] U.P. Hwang, K.F. Moran, Boiling heat transfer of silicon integerated circuits chip mounted on a substrate, Heat Transfer Electron. Equip. ASME HTD 20 (1981) 53–59.
[4] N.K. Phadke, S.H. Bhavnani, A. Goyal, R.C. Jaeger, J.S. Goodling, Re-entrant cavity surface enhancements for immersion cooling of silicon multichip packages, IEEE Trans. Compn. Hybrids Manufact. Technol. 15 (1992) 815–822.
[5] J.P. O'Connor, S.M. You, D.C. Price, A dielectric surface coating technique to enhance boiling heat transfer from high power microelectronics, IEEE Trans. Compn. Pack. Manufact. Technol. 18 (1995) 656–663.
[6] T.M. Anderson, I. Mudawar, Microelectronic cooling by enhanced pool boiling of a dielectric fluorocarbon liquid, ASME J. Heat Transfer 111 (1989) 752–759.
[7] H. Kubo, H. Takamatsu, H. Honda, Effects of size and number density of micro-reentrant cavities on boiling heat transfer from a silicon chip immersed in degassed and gas dissolved FC-72, J. Enhanced Heat Transfer 6 (1999) 151–160.
[8] S. Ujereh, T. Fisher, I. Mudawar, Effects of carbon nanotube arrays on nucleate pool boiling, Int. J. Heat Mass Transfer 50 (2007) 4023–4038.
[9] H. Honda, H. Takamastu, J.J. Wei, Enhanced boiling of FC-72 on silicon chips with micro-pin-fins and submicron-scale roughness, J. Heat Transfer 124 (2002) 383–390.
[10] J.J. Wei, H. Honda, Effects of fin geometry on boiling heat transfer from silicon chips with micro-pin-fins immersed in FC-72, Int. J. Heat Mass Transfer 46 (2003) 4059–4070.
[11] H. Honda, J.J. Wei, Enhanced boiling heat transfer from electronic components by use of surface microstructures, Exp. Thermal Fluid Sci. 28 (2004) 159–169.
[12] J.J. Wei, L.J. Guo, H. Honda, Experimental study of boiling phenomena and heat transfer performances of FC-72 over micro-pin-finned silicon chips, Heat Mass Transfer 41 (2005) 744–755.
[13] I. Mudawar, D.E. Maddox, Critical heat flux in subcooled flow boiling of fluorocarbon liquid on a simulated electronic chip in a vertical rectangular channel, Int. J. Heat Mass Transfer 32 (1989) 379–394.
[14] S.S. Kutateladze, B.A. Burakov, The critical heat flux for natural convection and forced flow of boiling and subcooled dowtherm, Problems of Heat Transfer and Hydraulics of Two-Phase Media, Pergamon, Oxford, 1989. pp. 63–70.
[15] K.R. Samant, T.W. Simon, Heat transfer from a small heated region to R-113 and FC-72, ASME J. Heat Transfer 111 (1989) 1053–1059.
[16] K.N. Rainey, G. Li, S.M. You, Flow boiling heat transfer from plain and microporous coated surfaces in subcooled FC-72, ASME J. Heat Transfer 123 (5) (2001) 918–925.
[17] S.J. Kline, F.A. McClintock, Describing uncertainties in single-sample experiments, Am. Soc. Mech. Eng. 75 (1953) 3–8.
[18] C.O. Gersey, I. Mudawar, Effects of orientation on critical heat flux from chip arrays during flow boiling, Trans. ASME J. Electr. Pack. 114 (1992) 290–299.
[19] K.M. Kirk, Jr.H. Merte, R. Keller, Low-velocity subcooled nucleate flow boiling at various orientations, ASME J. Heat Transfer 117 (1995) 380–386.